# *Supporting Information*

## Key-Enabled Molecular Rotation Modulates Intramolecular Hydrogen Bonding Toward a turn-on Trace-Level $N_2H_4$ Sensor

Dagang Shen [a, †], Chang Song, [a, †] Liqin Liu [a], Huabao Li [a], Yingying Ju [a], Weiwen Jing [a *], Huanhuan Wang [a *]

College of Chemistry and Chemical Engineering, Xinjiang Agricultural University, Urumqi 830002, China.

* Corresponding author.

E-mail address: wanghuanhuan@xjau.edu.cn (H.Wang).

**Table S1.** Photophysical properties of **SDG-2** in different solvents

| Probe | Solvent | $\lambda_{abs}$[(a)] | $\lambda_{em}$[(b)] | Δss/nm[(c)] | ε/$M^{-1}cm^{-1}$ [(d)] | $\Phi_f$[(e)] |
|---|---|---|---|---|---|---|
| SDG-2 | cyclohexane | 399 | 440 | 41 | 6000 | 72% |
| | Toluene | 400 | 450 | 50 | 3800 | 86% |
| | THF | 385 | 466 | 81 | 10600 | 38% |
| | Chloroform | 386 | 471 | 85 | 3600 | 37% |

**Table S2.** Comparison of other fluorescent probes with **SDG-2**- $N_2H_4$.

| Probe | Respond type | Detection media | LOD ($N_2H_4$) | Respond time | Ref. |
|---|---|---|---|---|---|
| HBA | Turn-on | HEPES | 0.43 μM | 10min | [1] |
| Myr-R | Turn-on | DMSO/$H_2O$ (3/7, v/v) | 3 nM | 20 min | [2] |
| Bz-PMA | Turn-on | THF | | 60 min | [3] |
| BBD | Ratiometric | DMSO/HEPES (9/1, v/v, *pH*= 7.4) | 0.1 μM | 28 min | [4] |
| T | Ratiometric | PBS | 0.25 μM | 10 min | [5] |
| MTT | Turn-on | DMSO/HEPES (9/1, v/v , *pH*= 7.4) | 0.37 μM | - | [6] |
| DQN | Turn-on | HEPES-DMF (4/6,v/v, pH 7.4) | 11.5 nM | 15 min | [7] |
| SDG-2 | Turn-on | DMSO/HEPES (9/1, v/v, *pH*= 7.4) | 0.43 μM | 10 s | This work |

## 1 Supplementary synthesis

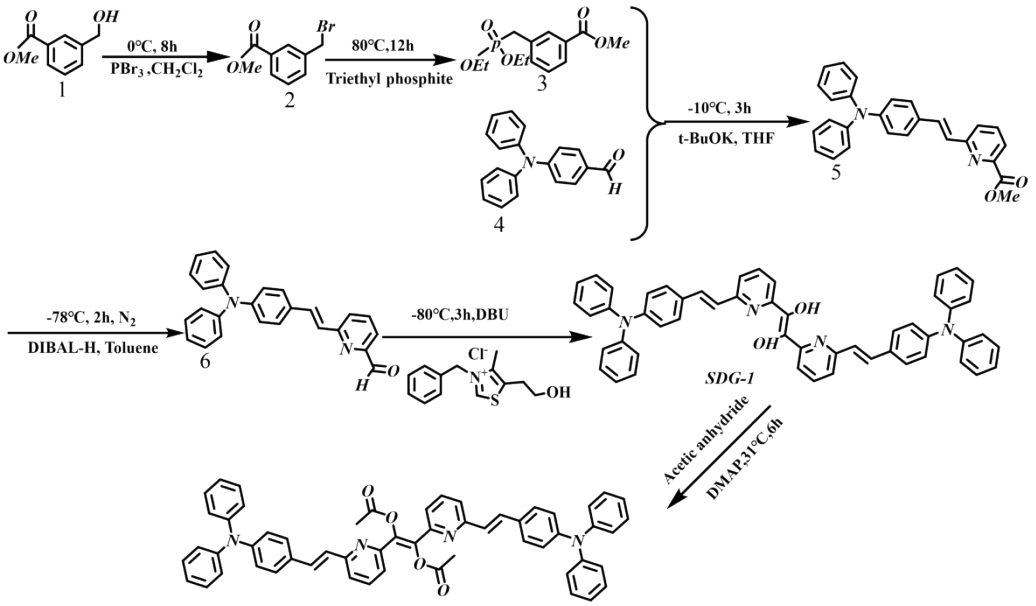


**Scheme S1**. Molecular synthesis route.

1.1 Synthesis of Compound 5

The compound diethyl (3-propylbenzyl)phosphonate was synthesized according to the reported method [9,10] and used directly in the next step reaction. A mixture of diethyl (3-propylbenzyl)phosphonate (300.0 mg, 1.04 mmol), 4-(diphenylamino)benzaldehyde (285.5 mg, 1.04 mmol), and potassium tert-butoxide (152.4 mg, 1.35 mmol) was dissolved in 15 mL anhydrous tetrahydrofuran. The mixture was stirred at 0°C until the starting material was totally consumed, as indicated by TLC. Four hours later, filtration and rotary evaporation removed the solvent to obtain a yellowish solid, which was separated by column chromatography (petroleum ether: dichloromethane = 3:1). The yield was approximately 62%.$^{1}$H NMR (400 MHz, $CDCl_3$) δ 7.91 (d, *J* = 7.5 Hz, 1H), 7.75 (t, *J* = 7.8 Hz, 1H), 7.60 (d, *J* = 7.8 Hz, 1H), 7.50 (d, *J* = 16.3 Hz, 1H), 7.41 (d, *J* = 8.6 Hz, 2H), 7.24 (s, 2H), 7.22 (s, 2H), 7.17 – 7.10 (m, 3H), 7.08 (s, 2H), 7.03 (d, *J* = 7.3 Hz, 2H), 7.00 (d, *J* = 3.7 Hz, 2H), 3.99 (s, 3H). $^{13}$C NMR (101 MHz, $CDCl_3$) δ 166.1, 156.8, 148.4, 147.9, 147.4, 137.4, 133.8, 130.0, 129.5, 128.3, 125.7, 125.0, 124.0, 123.5, 123.0, 122.8, 53.0. HRMS ($ESI^+$ ) calcd for $C_{27}H_{22}N_2O_2$ $[M+H]^+$ : 407.1715, found 407.1698. The Compound **5** structure was well demonstrated in terms of spectra of $^{1}$H NMR, $^{13}$C NMR, HRMS (ESI, m/z) (Fig. S1–Fig. S3)

1.2 Synthesis of Compound 6

The compound 5 (50.0 mg, 0.12 mmol) was dissolved in 25 mL of anhydrous toluene. Under nitrogen protection at -80°C, diisobutylaluminum hydride (7.5 mL, 41.6 mmol) was slowly added to the reaction mixture and stirred for 2 hours. Upon completion of the reaction, the reaction was quenched with 10 mL of methanol, followed by 100 mL of saturated sodium tartrate solution, and then stirred for another 2 hours. The organic phase was then extracted with ethyl acetate (20.0 mL × 3), dried over anhydrous magnesium sulfate, and the organic solvent was removed by rotary evaporation to yield a yellow solid. The crude product was purified by silica gel column chromatography (petroleum ether: dichloromethane = 1:2), resulting in the isolation of 27.2 mg of compound 6 as an orange-yellow solid, with a yield of approximately 88%.$^{1}$H NMR (400 MHz, $CDCl_3$) δ 10.11 (s, 1H), 7.80 (dd, *J* = 7.9, 4.5 Hz, 2H), 7.72 (s, 1H), 7.47 (d, *J* = 8.7 Hz, 2H), 7.30 (d, *J* = 1.9 Hz, 1H), 7.28 (dd, *J* = 6.9, 1.4 Hz, 4H), 7.15 (d, *J* = 1.1 Hz, 1H), 7.12 (t, *J* = 1.6 Hz, 2H), 7.09 (d, *J* = 4.6 Hz, 2H), 7.07 (d, *J* = 1.7 Hz, 2H), 7.05 (s, 2H). $^{13}$C NMR (101 MHz, $CDCl_3$) δ 194.0, 156.9, 152.7, 148.6, 147.4, 137.5, 134.1, 129.9, 129.5, 128.3, 125.6, 125.0, 123.6, 122.8, 119.5. HRMS ($ESI^+$ ) calcd for $C_{26}H_{20}N_2O$ $[M+H]^+$ : 377.1609, found 377.1594. The Compound **5** structure was well demonstrated in terms of spectra of $^{1}$H NMR, $^{13}$C NMR, HRMS (ESI, m/z) (Fig. S4–Fig. S6)

## 2 Supplementary methods

2.1 Detection limit

A fluorescence titration was carried out in HEPES buffer (10 mM, pH 7.4, 90% DMSO) to determine the detection limit, which was then calculated using the equation:

$$\mathbf{LOD = 3\sigma/K}$$

where σ is the standard deviation of the blank measurements and K is the slope between the intensity ratio and the sample

concentration.

2.2 Fluorescence quantum yield

This investigation, 9,10-diphenylanthracene was selected as the reference standard, which exhibits a reported fluorescence quantum yield of 0.95 in ethanol (n = 1.36) [44]. The reference (9,10-diphenylanthracene) and **SDG-2** were dissolved in anhydrous ethanol and dichloromethane (n = 1.42), respectively, and diluted to appropriate concentrations to ensure absorbance values below 0.1 at the excitation wavelength. The fluorescence quantum yields of the **SDG-2** were calculated using the following equation:

$$\Phi x = \Phi s(Fx/Fs)\ (Ax/As)$$

Φx and Φs are the fluorescence quantum yields of **SDG-2** and quinine sulfate, respectively. Fx and Ax represent the integrated fluorescence intensity and absorbance of **SDG-2**, respectively. Fs and As are the integral fluorescence intensity and absorbance of quinine sulfate, respectively.

2.3 Determination of Molar Absorptivity

A precisely weighed amount of **SDG-2** was dissolved in solvents of varying polarity to prepare stock solutions with a concentration of $1.0 \times 10^{-5}$ M. The UV-Vis absorption and fluorescence emission spectra of the dye solutions were subsequently recorded using a quartz cuvette with 1 cm optical path length. The molar extinction coefficient (ε) was calculated according to the Beer-Lambert law:

$$\varepsilon = A/(b \cdot c)$$

where ***A*** denotes the absorbance at the maximum absorption wavelength, ***b*** represents the cuvette path length (cm), and ***c*** corresponds to the molar concentration ($mol \cdot L^{-1}$).

2.4 The fluorescence detection of hydrazine in practical samples

In order to detect hydrazine from environmental, biological, plant, food samples, Three types of the real samples including the environmental sample such as soil and tap water, plant sample (Cabbage), food samples (seafood: fish; the regular food class: pork) were collected for the recovery experiments, which were under the pressure of hydrazine risk. These samples were from areas potentially affected by biogenic amine risks. The soil sample was collected from Xinjiang Agricultural University. Then, 0.1 g of the soil sample was added to 100 mL of pure water, stirred for 12 h, and subsequently filtered. Food samples, specifically seafood (Oreochromis) and common food items (pork), were collected from Xinjiang Agricultural University and a local supermarket, respectively. Next, 0.5 g of each sample was thoroughly mashed in a mortar and then added to 20 mL of concentrated nitric acid and left for 12 h. The resultant residues were then centrifuged at 8000 r/min in a centrifuge, and the obtained supernatant was used for the detection of hydrazine. Finally, the desired amounts of $N_2H_4$ (35 μM, 75 μM, 205 μM) were spiked into different real - world samples. After adding the probe **SDG-2** solution (λex = 390 nm) and incubating for 30 min, the recoveries of biogenic amines at various concentrations were determined. All

measurements were carried out in triplicate.

## 3 . $^{1}$H-NMR, $^{13}$C-NMR and HRMS analyses

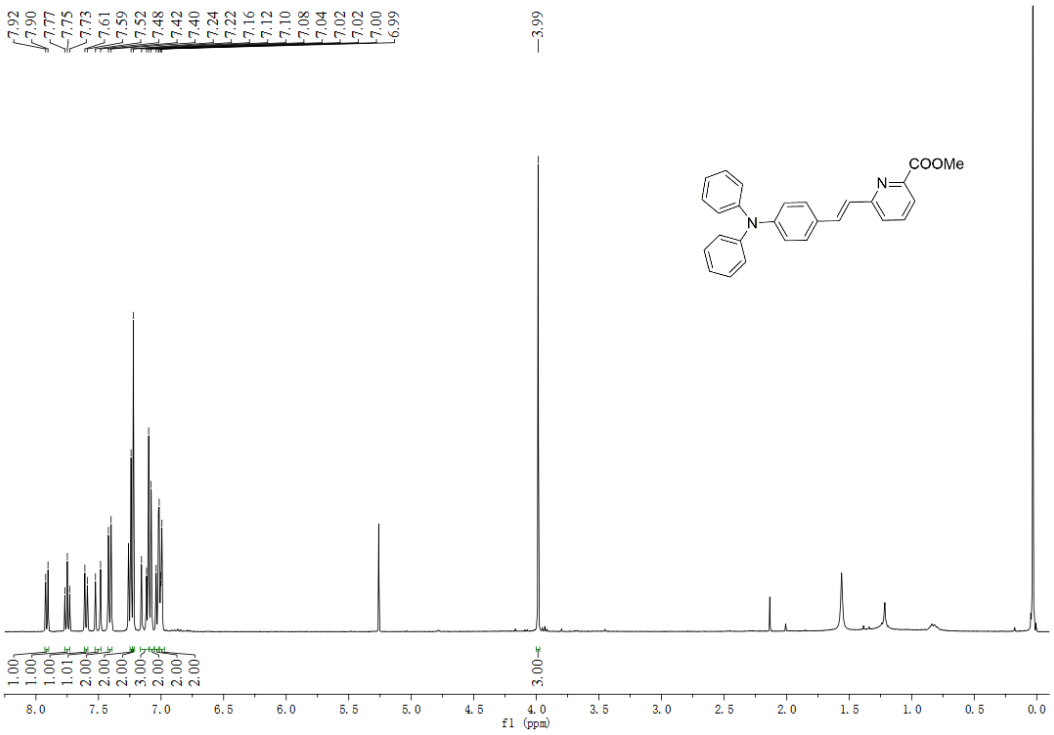


**Fig. S1.** $^{1}$H-NMR spectrum of compound 5 in $CDCl_3$

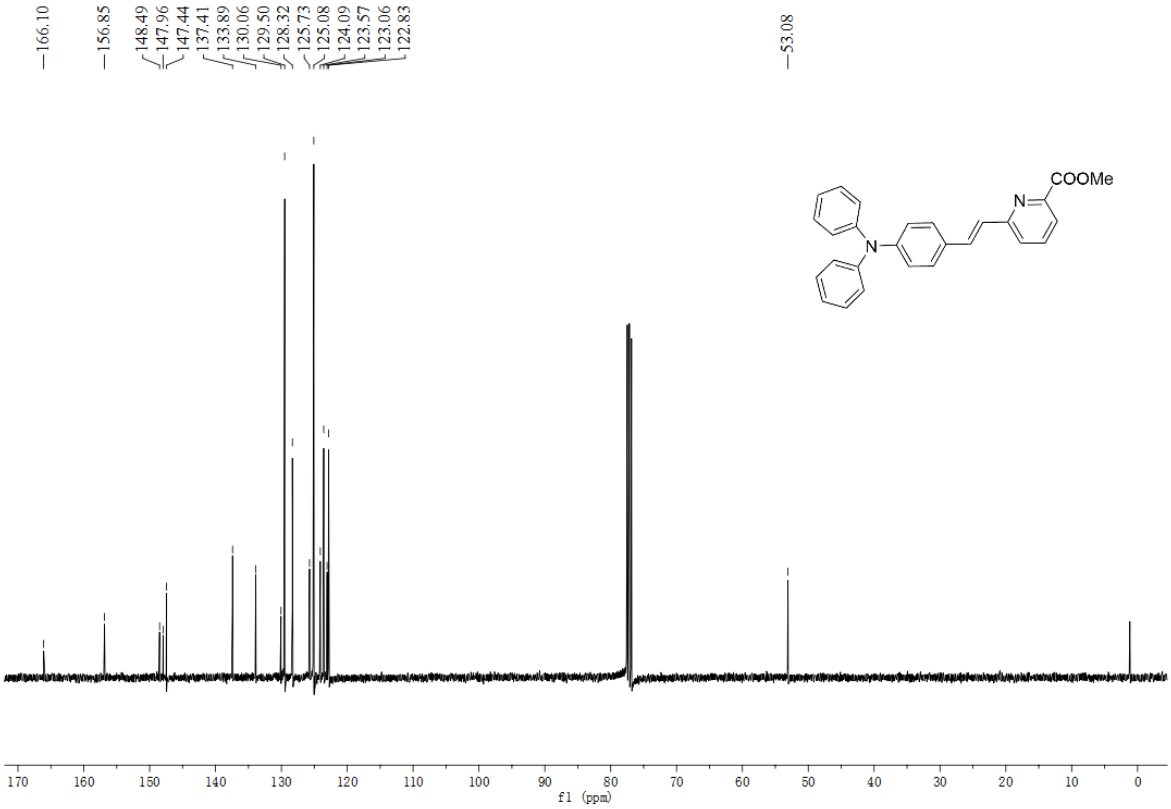


**Fig. S2.** $^{13}$C-NMR spectrum of compound 5 in $CDCl_3$.

81

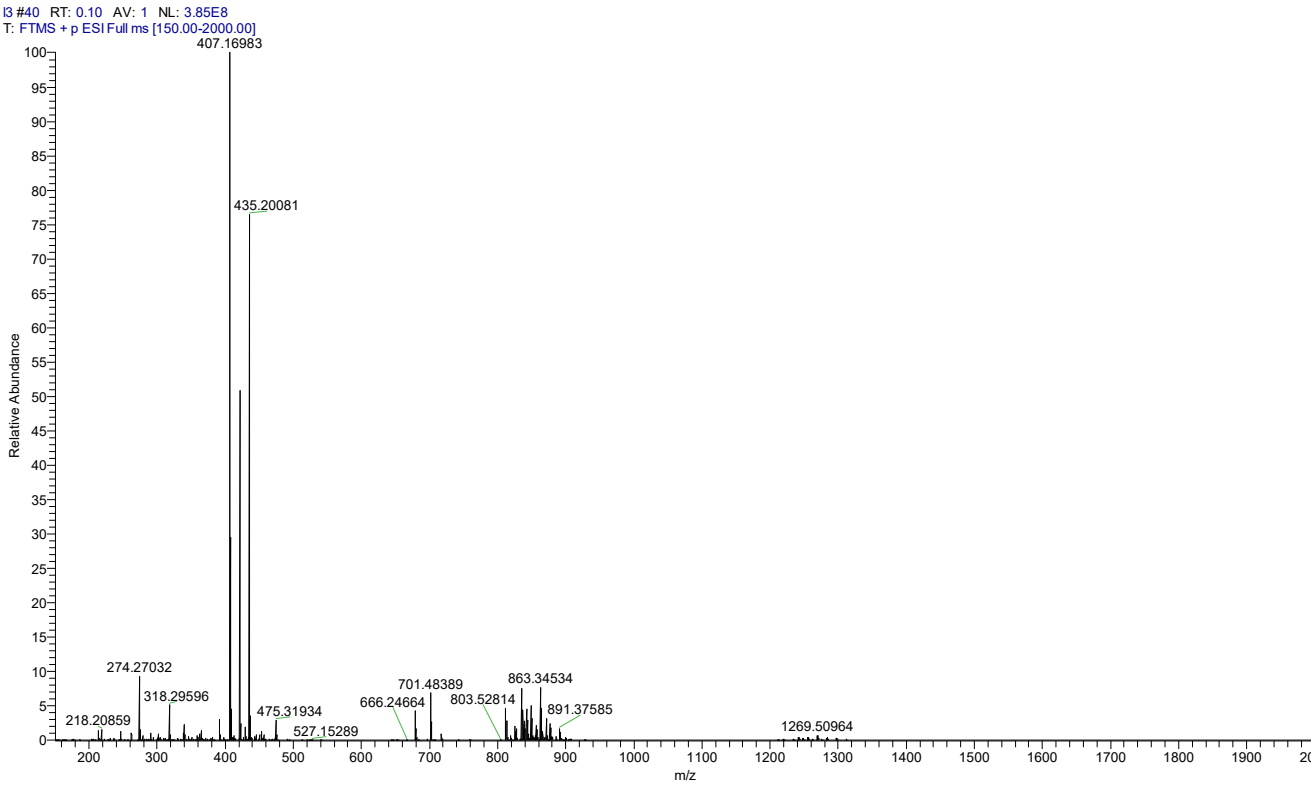


**Fig. S3.** HRMS spectrum of compound 5.

82

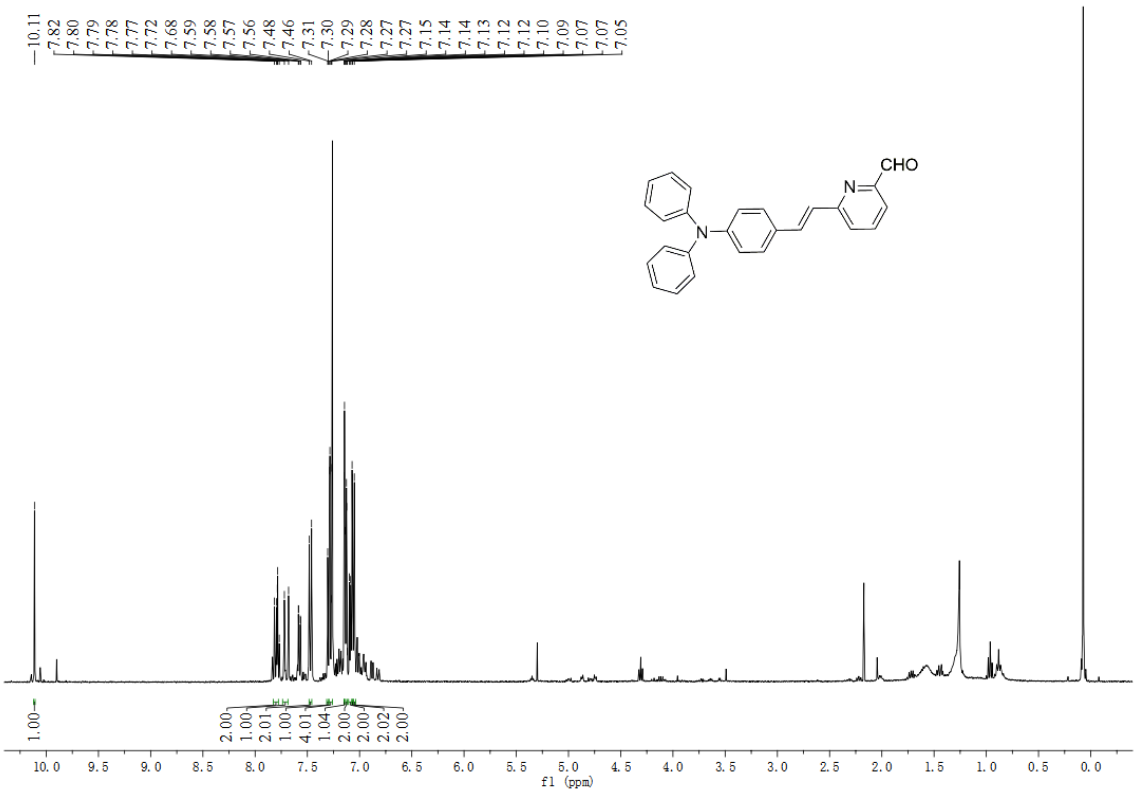


**Fig. S4.** $^{1}$H-NMR spectrum of compound 6 in $CDCl_3$.

83

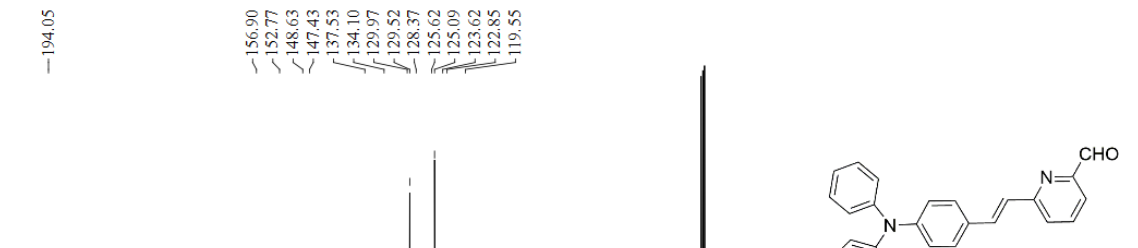

**Fig. S5.** $^{13}$C-NMR spectrum of compound 6 in $CDCl_3$.

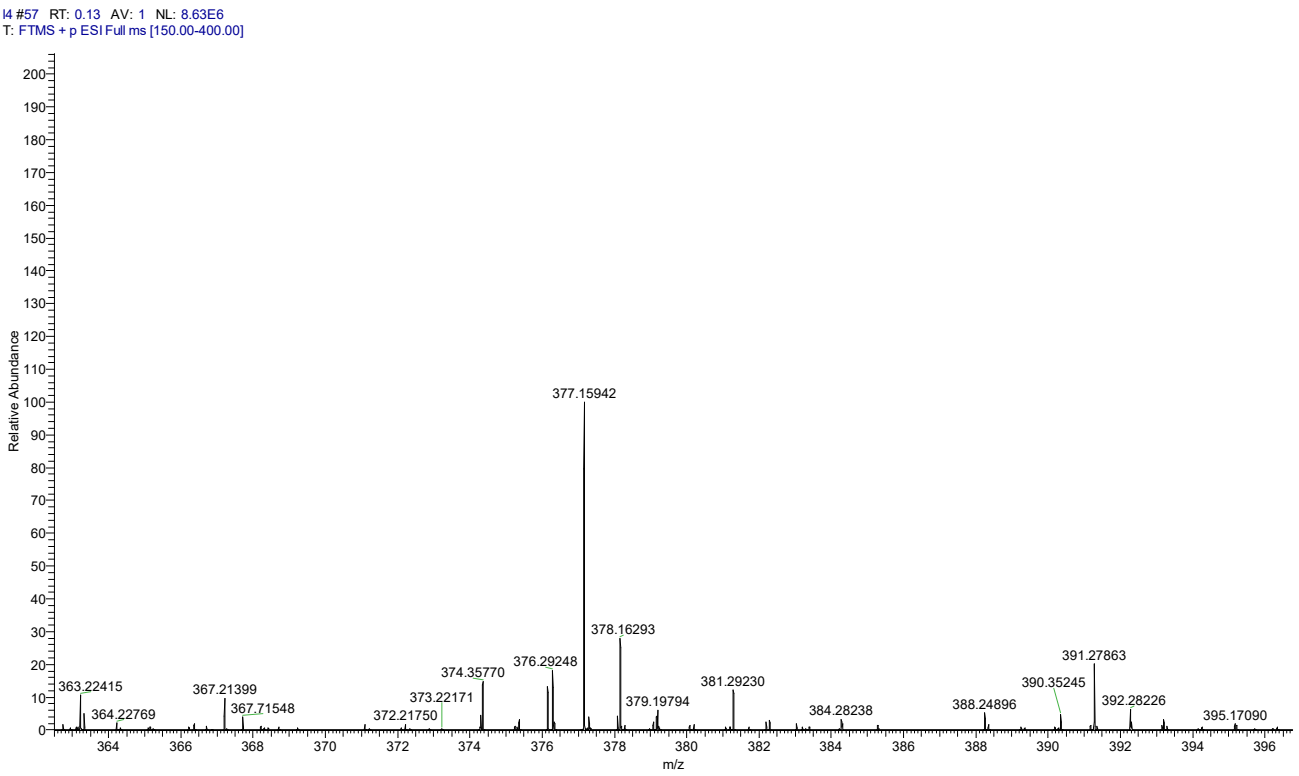


**Fig. S6.** HRMS spectrum of compound 6.

**Fig. S7.** $^{1}$H-NMR spectrum of **SDG-1** in $CDCl_3$.

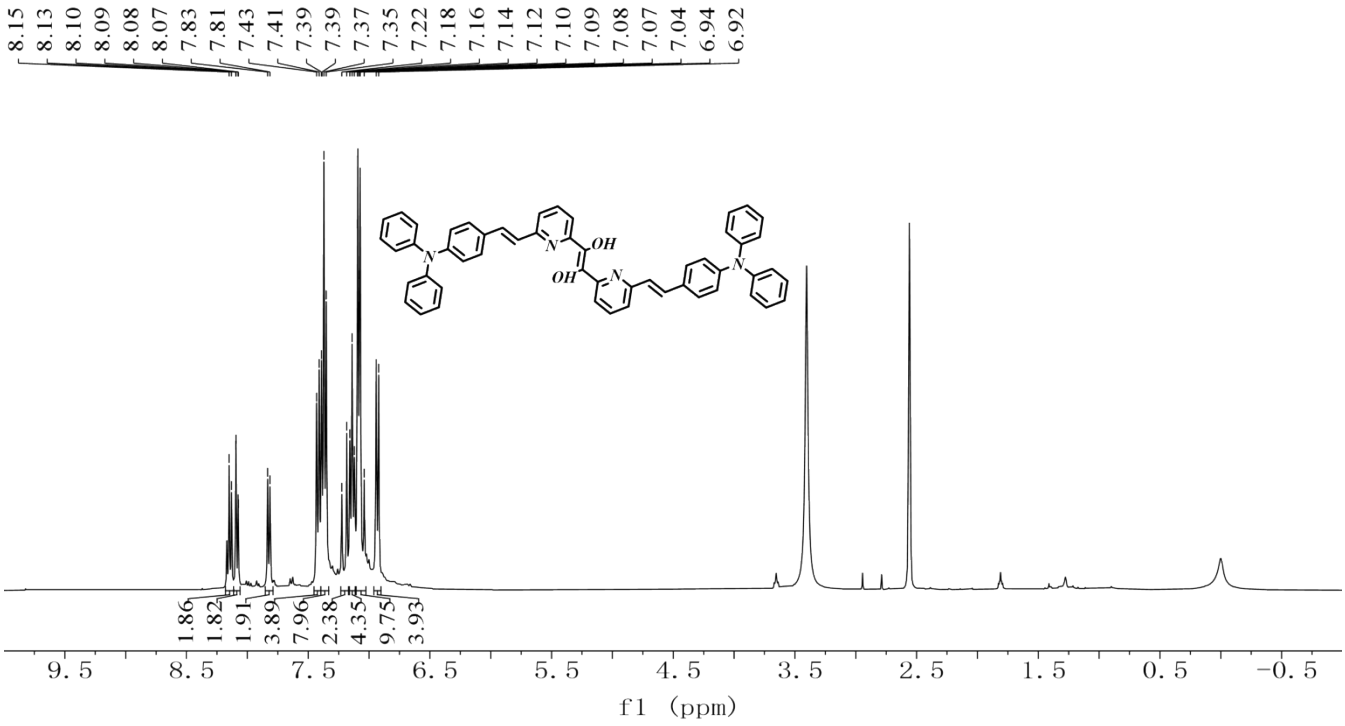

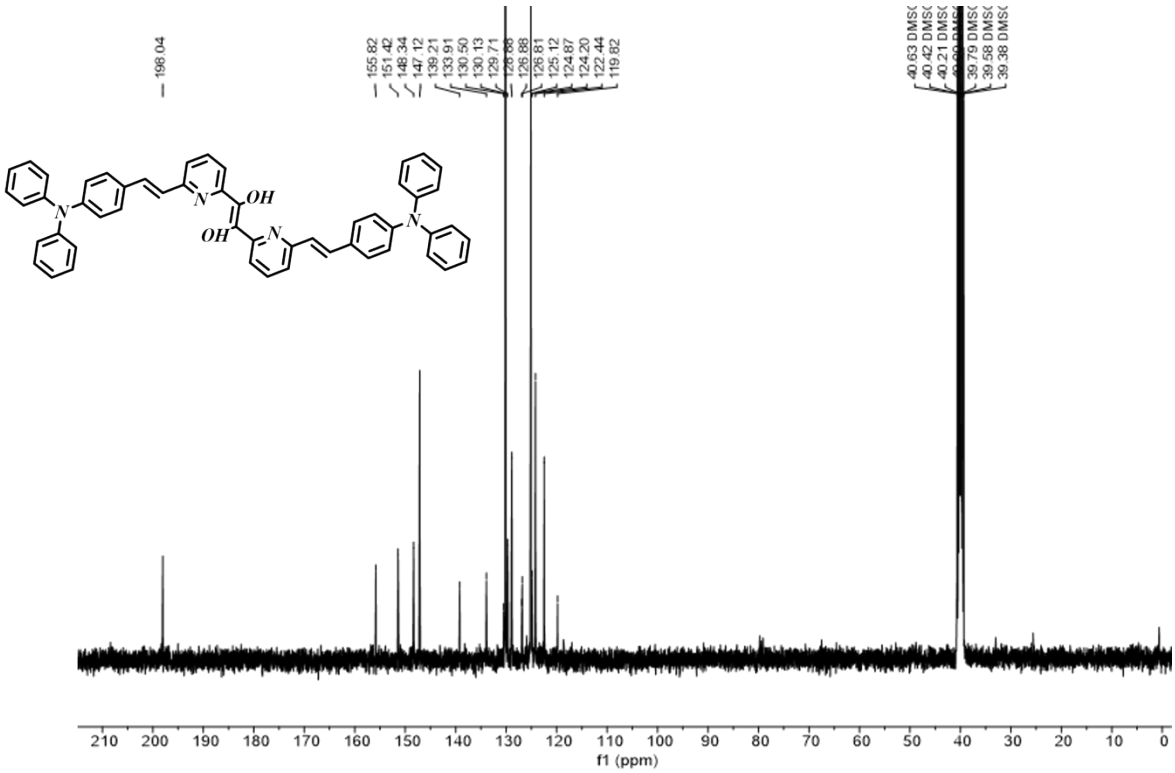


**Fig. S8.** $^{13}$C-NMR spectrum of **SDG-1** in CDCl3.

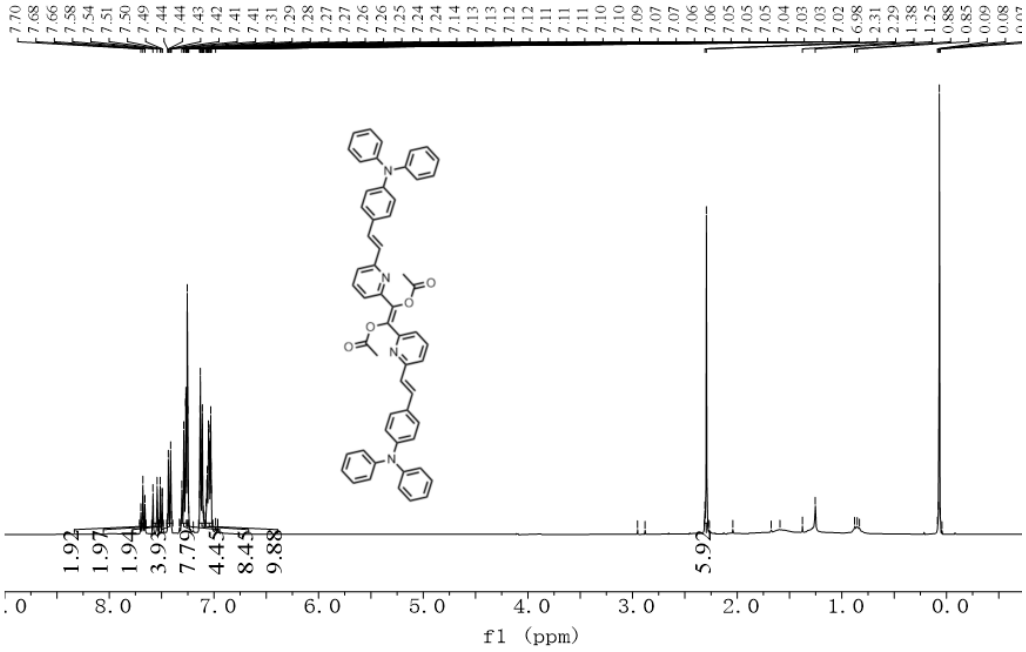


**Fig. S9**. $^{1}$H-NMR spectrum of **SDG-2** in $CDCl_3$.

90

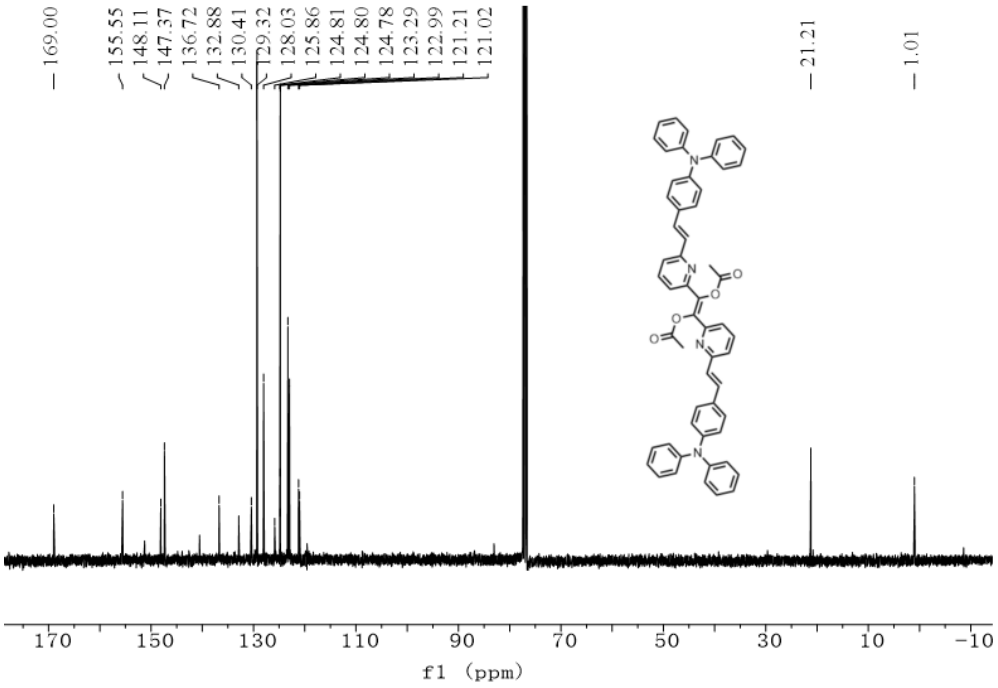


**Fig. S10** .[13]C-NMR spectrum of **SDG-2** in $CDCl_3$

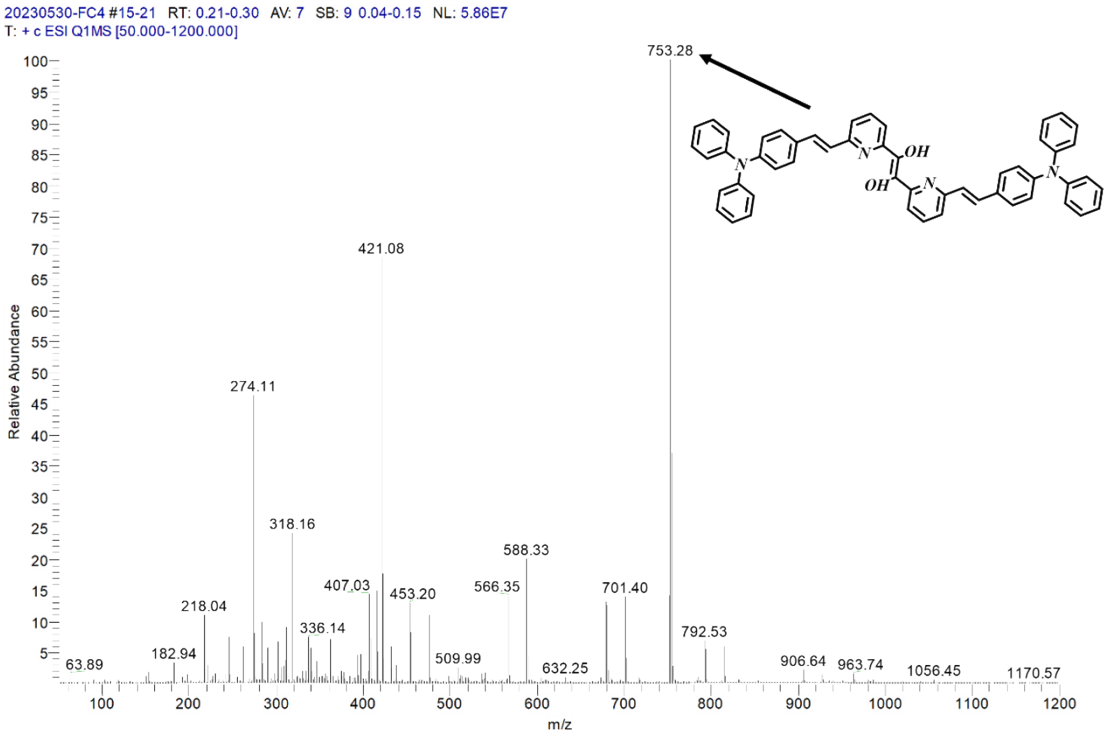

**Fig. S11**. MS ESI spectrum of SDG-1

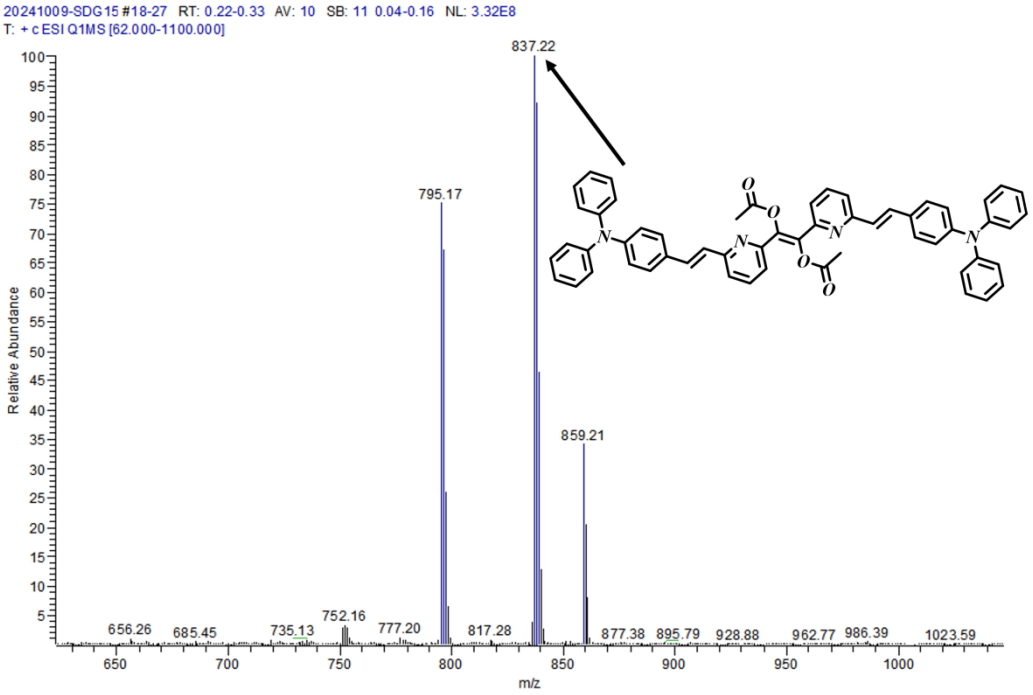


91

92 **Fig. S12.** MS ESI spectrum of SDG-2

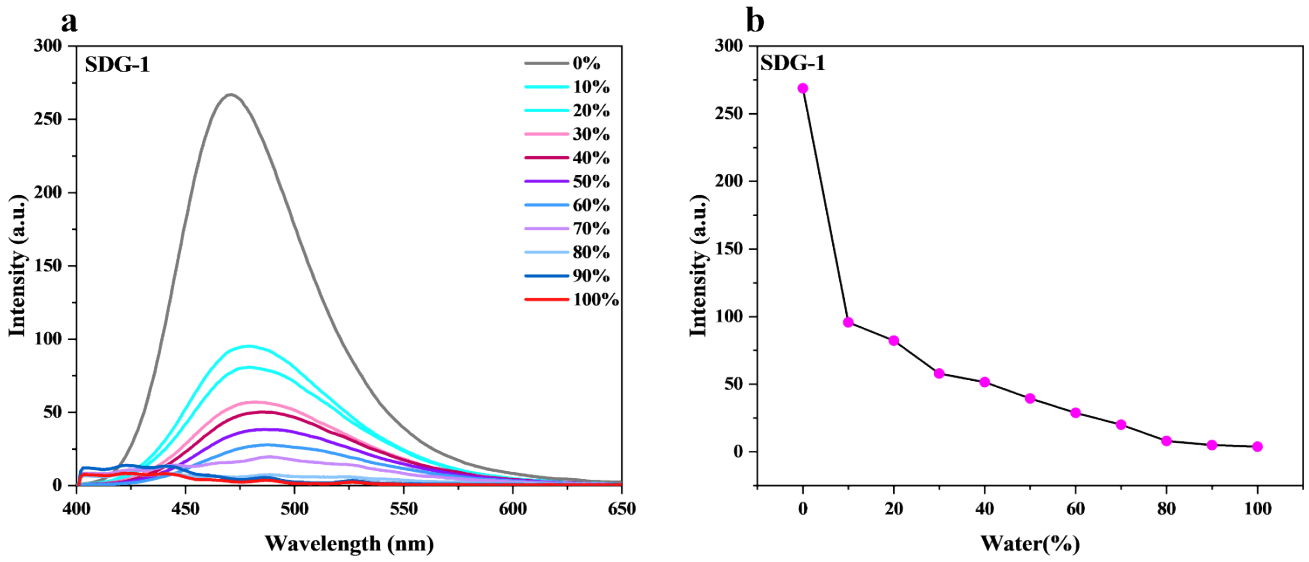


**Fig. S13.** (a) (a) Fluorescence emission spectra of compound SDG-1 (10 μM) in THF/$H_2O$ solutions with different volume ratios; (b) The relationship between fluorescence intensity and water fraction ($f_w$).

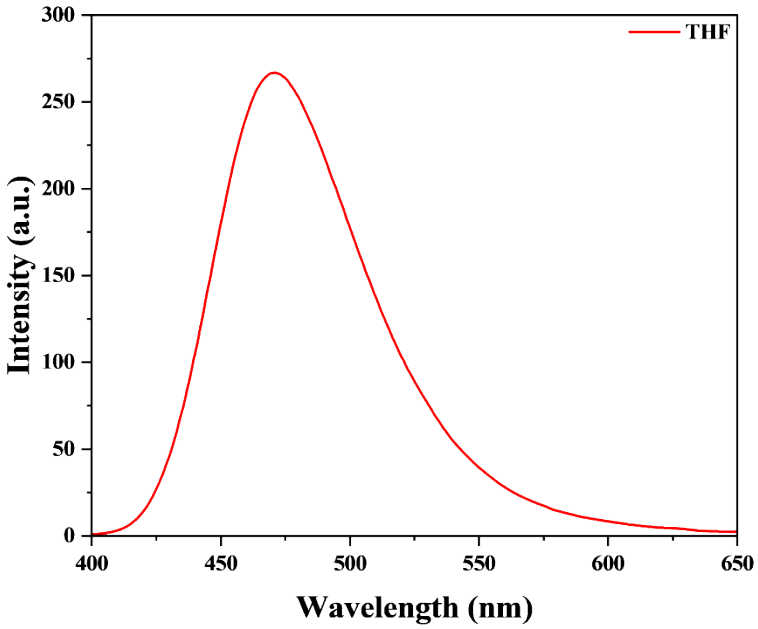


93

94 **Fig. S14** .The emission spectrum of **SDG-1** in tetrahydrofuran.

95

## 4 References


[1] S. Hu, J. Wang, M. Luo, Z. Wu, et al, A novel ESIPT fluorescent probe derived from 3-hydroxyphthalimide for hydrazine detection in aqueous solution and living cells, Analytical and Bioanalytical Chemistry, 413 (2021) 5463–5468. https://doi.org 10.1007/s00216-021-03530-1.

[2] W. Xiao, Q. Zhang, D.H. You, et al, Myricetin-based fluorescence probes with AIE and ESIPT properties for detection of hydrazine in the environment and fingerprinting, Analytica Chimica Acta, 1288 (2024) 342173. https://doi.org/10.1016/j.aca.2023.342173.

[3] M. Karman, E. Verde-Sesto, C. Weder, Mechanochemical activation of polymer-embedded photoluminescent benzoxazole moieties, ACS Macro Letters ,7 (2018) 1028–1033. https://doi.org /10.1021/acsmacrolett.8b00520.

[4] F. Fan, C. Xu, X. Liu, et al, A novel ESIPT-based fluorescent probe with dual recognition sites for the detection of hydrazine in the environmental water samples and in-vivo bioimaging, Spectrochimica Acta Part A: Molecular and Biomolecular Spectroscopy, 280 (2022) 121499. https://doi.org/10.1016/j.saa.2022.121499.

[5] Guan P, Yang B, Chai J, et al. A stable hydrazine click fluorescent probe based on photo switch. Dyes and Pigments, 2021, 186: 108983. https://doi.org/10.1016/j.dyepig.2020.108983.

[6] C. Liu, F. Wang, T. Xiao, et al. The ESIPT fluorescent probes for $N_2H_4$ based on benzothiazol and their applications for gas sensing and bioimaging, Sens. Actuators, B. 256 (2018) 55–62. https://doi.org/10.1016/j.snb.2017.09.198.

[7] G. Zhou, P. Ma, C. Yang, et al. A fluorescent probe based on modulation of ESIPT signaling for the highly selective detection of N2H4 and cell-imaging, Spectrochim. Acta. A. Mol. Biomol. Spectrosc, 303 (2023) 123233. https://doi.org/10.1016/j.saa.2023.123233.